RADIO SCIENCE, VOL. 37, NO. 3, 1031, 10.1029/2000RS002567, 2002

A direction-sensitive model of atmospheric noise and its application to the analysis of HF receiving antennas

C. J. Coleman

Electrical and Electronic Engineering Department, University of Adelaide, South Australia, Australia

Received 27 September 2000, revised 16 October 2001; accepted 16 October 2001; published 9 May 2002.

[1] Global maps of lightning occurrence are combined with ray tracing propagation calculations to form a direction-sensitive model of atmospheric noise. The model suggests a very complex directional behavior that can vary strongly with location, time, season, sunspot number, and frequency. It is shown that the directional variability of noise, when coupled with the directional variability of antenna gain, can lead to marked changes in noise outcome between different antennas. The implication of directional varying noise for the optimum choice of receiver antenna is explored. *INDEX TERMS:* 6964 Radio Science: Radio wave propagation; 0609 Electromagnetics: Antennas; 6914 Radio Science: Electromagnetic noise and interference; *KEYWORDS:* radio noise, atmospheric noise, noise modeling

1. Introduction

[2] A radio receiving system is ideally designed so that the external noise environment is the only limit to the signals that can be received (i.e., the system is externally noise limited). At HF the principal components of the external noise are galactic, man-made, and atmospheric in origin. All of these components exhibit variations with frequency, but atmospheric noise can also have strong variations with respect to location, season, and time. During the daytime, noise is at its lowest level, with strong ionospheric absorption removing most of the nonlocal atmospheric component on the lower HF frequencies. At night, however, absorption is greatly reduced, and noise levels can rise considerably. In particular, noise from thunderstorms (the dominant source of atmospheric noise) can propagate very effectively via the ionosphere and, as consequence, make contributions on a global scale.

[3] The standard HF noise model is that produced by the *International Telecommunication Union* (*ITU*) [1999]. This is based on observations from a limited number of stations and tends to provide a fairly coarse picture of noise distribution. *Kotaki* [1984] has shown that model estimates of noise can be greatly improved if the atmospheric contributions are calculated from global maps of thunderstorm activity [*Kotaki and Katoh*, 1984] by means of suitable propagation calculations. It should be noted, however, that the noise models of both Kotaki and the International Radio Consultative Committee (CCIR) fail to provide information about directional variations. That atmospheric noise must be highly directional is clear from the significant global variation of thunderstorm activity. Furthermore, a strong directional dependence is supported by observations using directional arrays [*Keller*, 1991].

[4] It is the purpose of the current paper to describe a model of atmospheric noise that addresses the directional issue. *Kotaki* [1984] employed a simple estimate of propagation effects, but the current work uses a far more sophisticated propagation model [*Coleman*, 1998]. Such an approach allows for the effects of anomalous propagation (transequatorial propagation, for example) and is essential if an accurate estimate of noise distribution, in terms of both azimuth and elevation, is to result. Another issue to be considered in this paper is the impact of directional noise upon antenna performance. For noise that is directional-dependent the total noise entering a receiver will depend on the directional properties of the antenna. Consequently, although it might seem sensible to choose the antenna that has maximum directivity for the desired signal, it is also possible that this antenna also has a strong response in directions from which the strongest noise arrives. The possible importance of the directional properties of noise has been raised by *CCIR* [1964] and is supported by some preliminary modeling results given by *Coleman* [2000]. The current paper gives a full account of the model used by Coleman and explores the implications of such a model for the optimum choice of receiver antenna.

Copyright 2002 by the American Geophysical Union.
0048-6604/02/2000RS002567$11.00

[5] Section 2 of this paper develops a directional noise model that is suitable for the above purposes. The section includes some examples of noise predictions for a variety of receiver sites and considers the effect of anomalous propagation upon the noise distribution. Section 3 of this paper considers the effect of directional noise upon antenna performance. It is demonstrated that the directionality of noise, when coupled with the directionality of the receiving antenna, can result in noise levels far different from those observed using a simple monopole antenna. Such a result has important implications for the planning of communication systems. The planner is normally forced to rely on predictions produced by the CCIR model, a model that assumes that the noise collected by a monopole is appropriate whatever the antenna system. As a consequence, the current noise model has been developed into a full communication prediction tool that incorporates the effects of antennas and directional noise. Section 4 draws some conclusions from the work and suggests some future developments.

2. Directional Noise Model

[6] The major source of atmospheric noise is lightning strikes. These can occur anywhere across the globe but are most frequent over the major landmasses. As pointed out by *Kotaki* [1984], their contributions to noise will consist of an ionospheric component (the radio energy of lightning that propagates via the ionosphere) and a local component (that which propagates directly or by ground waves). The ionospheric component is the combination of energy from many random discharges across the globe and results in a fairly constant drizzle of noise. As such, the ionospheric component sets the lower limit of noise at any site. The local component is more erratic in nature and consists of isolated bursts of noise from local strikes (those within a few hundred kilometers of the receiver). While increases in computing power might eventually allow the local noise to be excised by means of adaptive nulling [*Carhoun*, 1991], the ionospheric component will always place a limit on the performance of an HF system.

[7] The more or less continuous nature of ionospheric noise density allows a model of this aspect to be derived from global maps of lightning strike rates (the local component needs to be dealt with in terms of the probability of noise bursts). In the current work, the model is based upon the strike rate database developed by *Kotaki and Katoh* [1984]. (This has been transformed into a suitable computer subroutine, and a sample lightning map is shown in Figure 1.) Consider the atmospheric noise that enters the receiver antenna through an infinitesimal solid angle at elevation θ and azimuth ϕ. For a given frequency the ionospheric propagation in this direction will either penetrate the ionosphere (i.e., a path for the very much weaker galactic noise) or be refracted back to the ground (a path for long-range atmospheric noise). By further reflections from the ground and ionosphere the propagation is extended until it either penetrates the ionosphere or the amplitude of the signal becomes negligible through various loss mechanisms. The major loss mechanisms are spreading loss, ionospheric absorption, and reflection loss. For ionospheric noise, however, the spreading loss is partly compensated for by the variation in area from which the noise is gathered. For a given solid angle at the receiver, the area from which noise is collected increases inversely with the spreading loss. The result is that the noise density N (watts per hertz per steradian) is given by

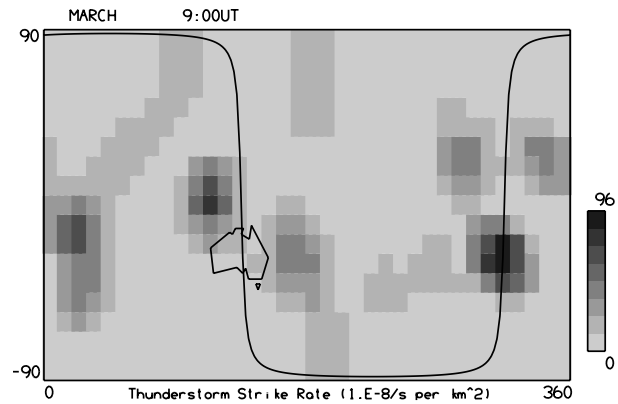

Figure 1. Global picture of lightning strike rates at 0900 UT. Read 1.E-8 as 1×10^{-8}.

$$N(\theta,\phi) = \sum WS\left(\frac{\lambda}{4\pi}\right)^2 \frac{1}{L\sin(\varphi)}, \qquad (1)$$

where W is the radiated energy density (joules per hertz) of a lightning strike, S is the strike rate (strikes per second per unit area) at the start point of the propagation path, φ is the elevation at which the propagation is launched, λ is the propagation wavelength, and L is the loss due to ground reflection and ionospheric absorption. It should be noted that the summation is over all possible lightning source regions that can propagate into the receiver from the given direction. (Note that equation (1) must be modified for energy launched at grazing angles). Data

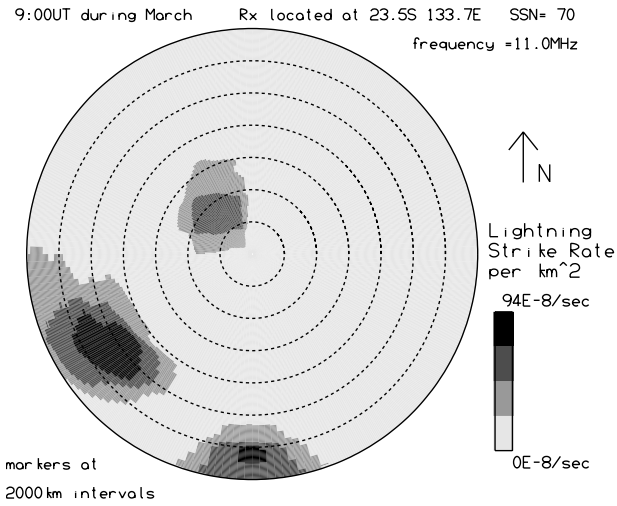

Figure 2. Lightning strike rates at dusk, centered on Alice Springs. SSN, sunspot number.

given by *Jursa* [1985] suggest a value of 2×10^{-6} J/Hz for W at 10 MHz and 10^{-5} J/Hz at 2.5 MHz.

[8] An important aspect of the noise model is the ionospheric propagation tool that is used to estimate the origin of energy arriving from a particular direction. This tool is described by *Coleman* [1998] and employs a two-dimensional (2-D) ray tracing tool together with an ionospheric model [*Coleman*, 1997] in which the electron density is described by Chapman layers and layer parameters are derived from the parameter maps of the international reference ionsophere 1990 model [*Bilitza*, 1990]. Propagation calculations also provide the information that is required to estimate the various losses. The ground reflection part of the loss L is given by

$$L_r = 10 \log_{10} \left(\frac{|R_v|^2 + |R_h|^2}{2} \right), \tag{2}$$

where

$$R_v = \frac{n^2 \sin\varphi - (n^2 - \cos^2\varphi)^{1/2}}{n^2 \sin\varphi + (n^2 - \cos^2\varphi)^{1/2}},$$

$$R_h = \frac{\sin\varphi - (n^2 - \cos^2\varphi)^{1/2}}{\sin\varphi + (n^2 - \cos^2\varphi)^{1/2}},$$

with $n^2 = \varepsilon_r - j18{,}000\sigma/f$, where ε_r is the relative dielectric constant of the Earth surface (80 for sea and an assumed value of 15 for land), σ is the conductivity of the surface (5 S/m for sea and an assumed value of 0.01 S/m for land), and f is the propagation frequency. In addition, the part of L due to ionospheric absorption is calculated from the expression [*Lucas and Haydon*, 1966]

$$L_a = \frac{677.2[\exp(-2.937 + 0.8445 f_0 E) - 0.04]}{\left[(f + f_L)^{1.98} + 10.2\right] \cos\phi_{100}}, \tag{3}$$

where f_L is the gyrofrequency, f_0E is the E region critical frequency, and ϕ_{100} is the angle between the propagation path and the vertical at an altitude of 100 km. The above expression accounts for the absorption in the D and E regions, but there will also be considerable deviative absorption in the F region for some propagation. In the present work, this additional absorption is estimated according to $0.01(P' - P)$ [*Davies*, 1990], where P' and P are the group and phase paths, respectively. (Note that L_r and L_a are given in terms of decibels.)

[9] Figure 2 shows the distribution of lightning strikes during dusk (0900 UT) for ranges up to 14,000 km out from Alice Springs (central Australia). The circles on the map denote range intervals of 2000 km, and strong lightning sources in the equatorial regions of America, Africa, and Southeast Asia will be noted. Figure 3 shows the resulting noise distribution over the skyward hemisphere for a frequency of 11 MHz, as calculated by the above model. The Southeast Asian sources result in strong noise from northwesterly directions, but it is clear that ionospheric propagation limits the noise to the lower elevations. Fairly strong noise is also evident from the east and southeast, and this is a result of good nighttime propagation across the Pacific Ocean. This propagation causes the low-level sources in this region to have an

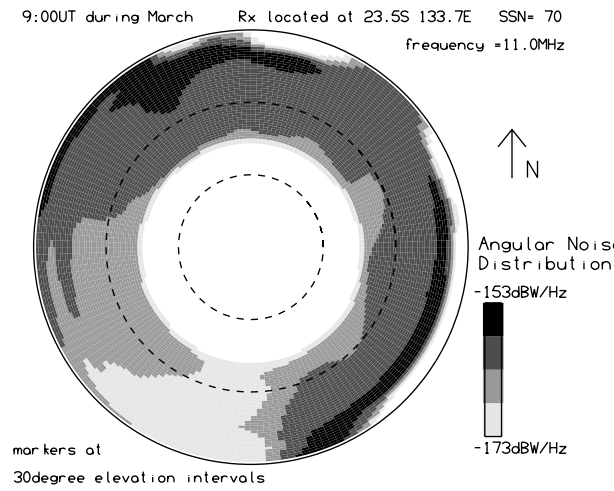

Figure 3. Directional noise distribution, as seen from Alice Springs at dusk.

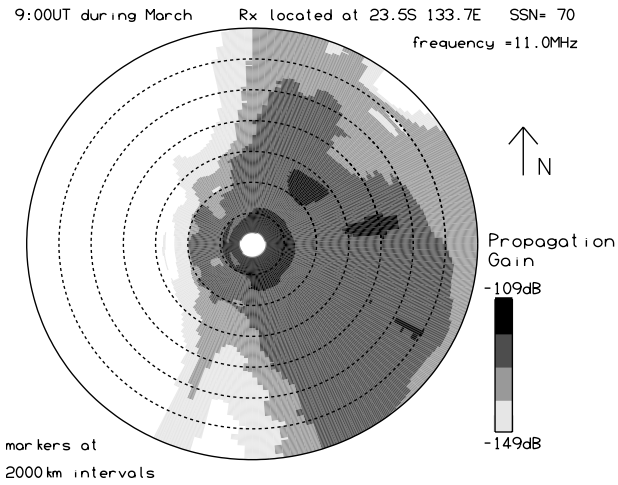

Figure 4. Propagation gain for signals reaching Alice Springs at dusk.

appreciable cumulative effect. Since radio waves from sources in the direction of Africa must travel through a significant amount of daylight, this noise is heavily reduced by absorption. Consequently, there is very little noise from the southwest sector. The effect of the losses can be better seen in Figure 4, which shows the propagation gain (the combined effect of propagation losses such as spreading, absorption, and reflection) for transmissions from points out to 14,000 km. The above simulations are supported by limited directional noise observations performed using the frequency management system of the Jindalee over the horizon radar at Alice Springs (P. S. Whitham, Defense Science and Technology Organisation

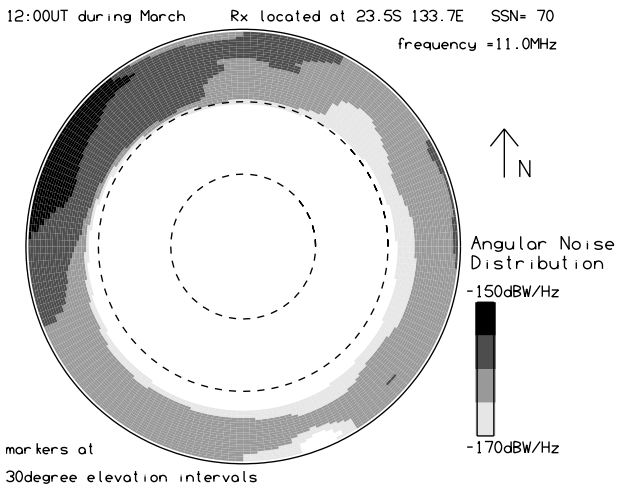

Figure 5. Directional noise distribution, as seen from Alice Springs in midevening.

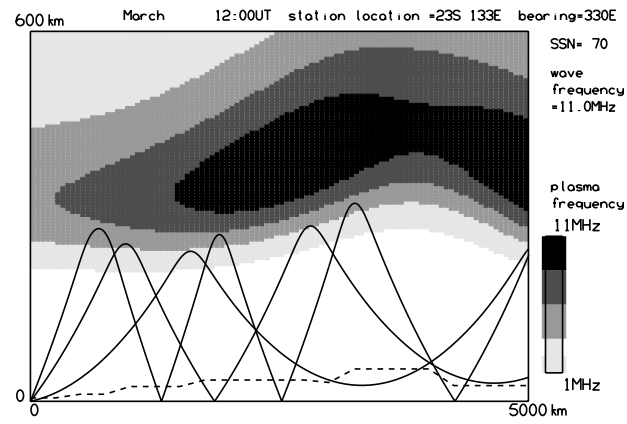

Figure 6. Propagation paths from Alice Springs to lightning sources.

Australia, private communication, 2000). These observations also show the strongest noise coming from the northwest and southeast sectors with total variations of more than 10 dB in azimuth. Figure 5 shows the simulated noise distribution for a time later in the evening (1200 UT), from which it will be noted that there is increased noise from Southeast Asia (to the northwest) due to the increased nighttime propagation in this direction.

[10] Figure 6 shows some typical propagation paths to the lightning sources in Southeast Asia (all of them exclusively in nighttime and so little affected by absorption). The dashed curve indicates the lightning strike rate, from which it is clear that there are good propagation paths to the most active regions. This is not always the case, as is illustrated by Figure 7. This figure shows propagation from Darwin, in the north of Australia, toward Southeast Asia. It will be noted that the effect of the equatorial anomaly (the peaks of electron density to the north and south of the geomagnetic equator) is to cause a considerable portion of the propagation to skip over the major thunderstorm sources. This will result in noise holes at low elevations, as can be seen from the directional noise distribution of Figure 8. The requisite chordal propagation is a well-established, and frequent, phenomenon in equatorial regions [*Davies*, 1990], and so the possibility of such holes is strong. If they exist, they could offer the possibility of low-power long-range communication for a system with suitably limited elevation response.

[11] An additional example of a noise distribution is shown in Figure 9. The figure shows the simulated noise for a receiver location slightly to the northwest of Boston (United States) during a winter morning. This simulation was chosen to coincide with the data collected by *Keller*

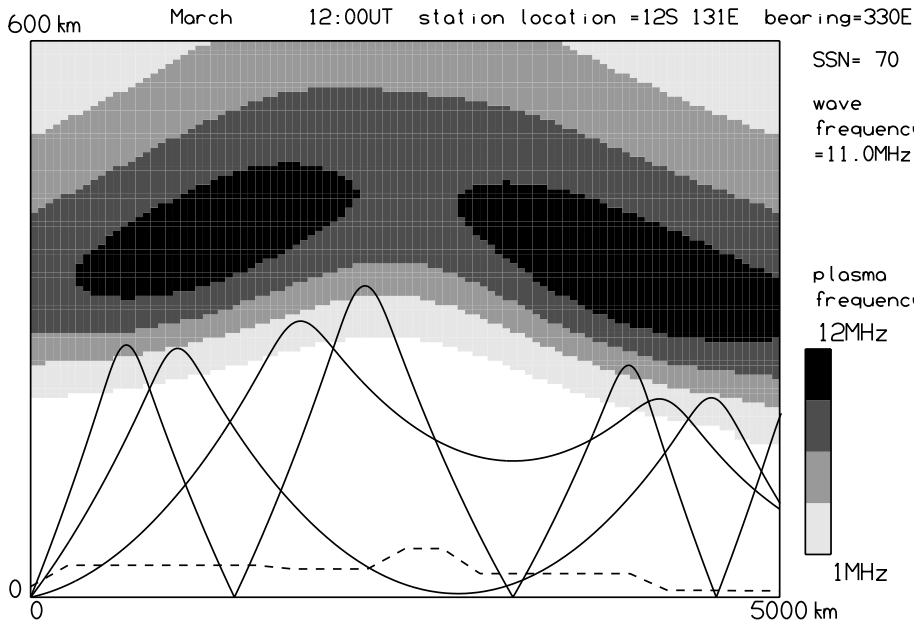

Figure 7. Propagation paths from Darwin to lightning sources.

[1991] on an L-shaped directional receiving array. This array geometry allowed Keller to infer the distribution of noise over the skyward hemisphere. It will be noted that the simulations show strong noise sources to the south and to the northwest, but much reduced noise in the northeast. This result is consistent with the observations of Keller and strongly suggests that much of the observed noise was atmospheric in origin. The simulated results also show the atmospheric noise to be confined to elevations below about 45°, strongly supporting Keller's inference that the higher noise levels were caused by energy arriving through ionospheric reflections. Figure 10 shows the lightning sources that contribute to the observed noise. It will be noted that there is a strong density of strikes immediately to the south. The effect of these sources will, however, be moderated by strong daytime ionospheric absorption. Other sources farther to the south and west will require several ionospheric hops to

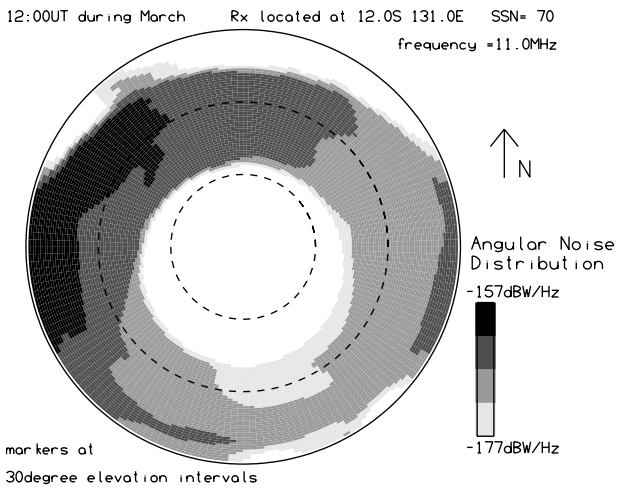

Figure 8. Directional noise distribution, as seen from Darwin in midevening.

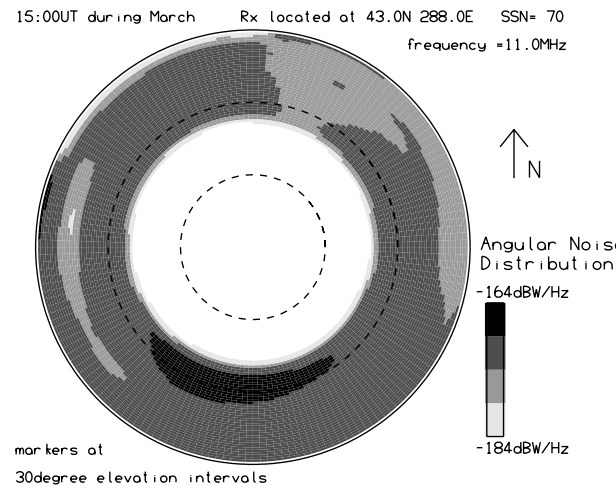

Figure 9. Directional noise distribution, as seen from Boston in the morning.

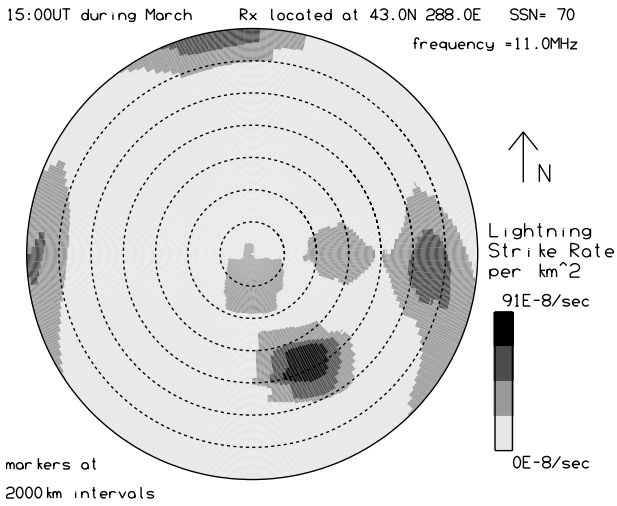

Figure 10. Lightning strike rates in the morning, centered on Boston.

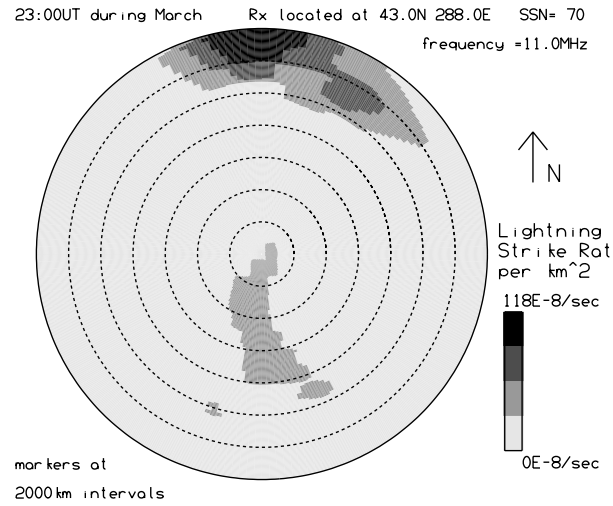

Figure 12. Lightning strike rates at dusk, centered on Boston.

reach the receiver and so will be even more heavily attenuated. Consequently, even though there are extremely strong thunderstorm regions in South America, these will have very little impact upon the noise spectrum at this time of day. While the sources in the northeast quadrant have a much lower strike rate than those immediately to the south, the closer proximity to the day/night transition will mean much lower signal attenuation and hence a significant contribution to the noise environment. The simulations of Figure 9 refer to a time that is well after dawn, and the daytime attenuation has much reduced the possible effects of ionospherically propagated noise. As a consequence, the azimuthal variation of noise is little more than 5 dB. For the same site at dusk, however, the attenuation is very much reduced, and lighting sources from much further afield can make a significant impact. Figure 11 shows the simulated noise distribution at this time, and Figure 12 shows the lightning distribution from which it originates. It can be seen that noise sources in Asia (across the pole) have a significant impact and that the good nighttime propagation across the Atlantic Ocean causes the low-level sources in this region to have an appreciable cumulative effect. To the west, however, the daytime conditions cause severe attenuation and hence result in very little noise (the total azimuthal variation of noise is now more than 10 dB).

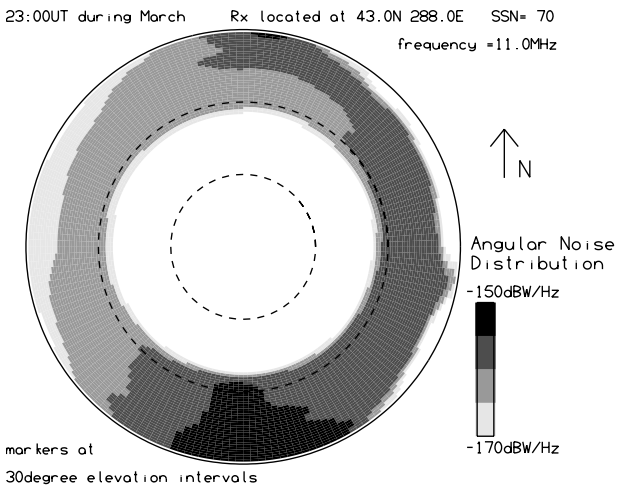

Figure 11. Directional noise distribution, as seen from Boston at dusk.

3. Some Antenna Considerations

[12] The strong directional dependence of noise raises the possibility that the directional properties of an antenna might significantly alter the amount of noise that is delivered to the receiver. It is possible that the antenna with maximum signal-to-noise ratio (SNR) for a particular signal might not correspond to the antenna with maximum directive gain in the direction of that signal. Consider three common HF antennas (a horizontal log-periodic antenna (HLPD), a horizontal travelling wave dipole (TWD), and an elevated feed monopole (EFM)) with the gain patterns shown in Figure 13. These antennas exhibit markedly different performance with respect to elevation and so will be appropriate for different ranges. Figure 14 shows the takeoff angles (TOAs) for strongest returns at a variety of ranges and azimuths (conditions are as in Figure 3). It will

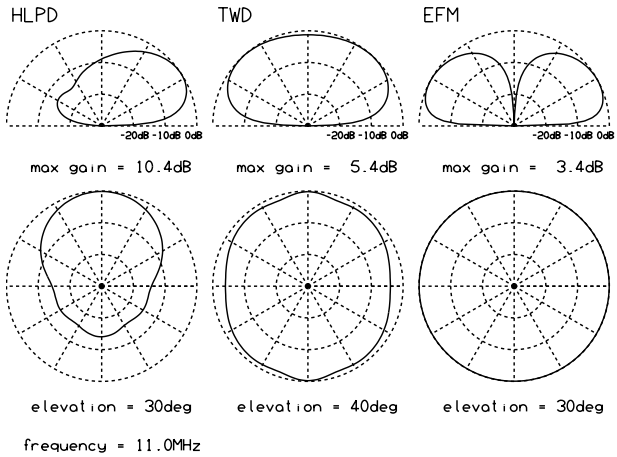

Figure 13. Gains for a variety of popular HF antennas.

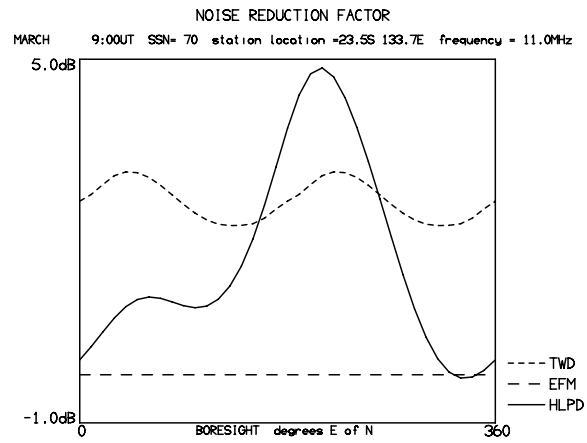

Figure 15. Dusk NRFs for various antennas at Alice Springs.

be noted that the HLPD antenna is appropriate for the longer ranges, the TWD is appropriate for the shorter ranges, and the EFM is appropriate for all ranges. The strongest atmospheric noise enters though the lower elevations since this propagation allows noise to be accumulated over a vast area. Consequently, the TWD will produce a much lower level of noise because of its very poor response at these lower elevations. In the case of the HLPD its strong azimuthal dependence will mean that when this antenna points away from the major noise sources, there will be a much lower level of total noise. Unfortunately, the downside is a much increased level of total noise when the antenna points toward the major noise sources. The EFM has a good response toward all noise sources and so has the poorest noise performance of all these antennas. The above conclusions are best illustrated through the noise reduction factor (NRF), the amount by which the noise entering the receiver is reduced from that collected by a monopole of the type used in the development of the CCIR database [*Clarke*, 1960]. This factor will vary with antenna type, location, boresight, frequency, time, season, and sunspot number. Figure 15 shows the NRF for a variety of antennas during dusk at Alice Springs. It will be noted that the NRF for the HLPD shows a very strong azimuthal dependence with largest values when the antenna points toward the southwest (the direction of least noise sources) and lowest values when it points toward the northwest (the direction of strongest noise sources). As expected, the TWD exhibits a large value of NRF with very little boresight variation, and the

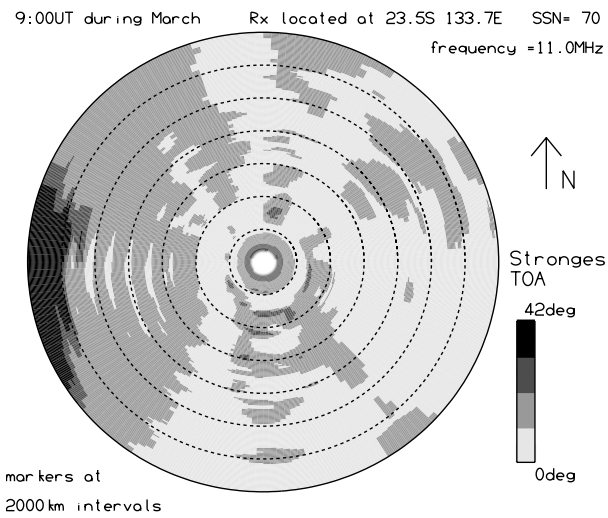

Figure 14. Map of TOAs for dusk at Alice Springs.

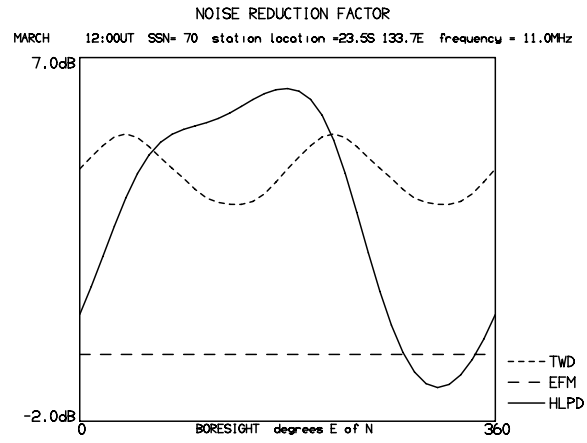

Figure 16. Midevening NRFs for various antennas at Alice Springs.

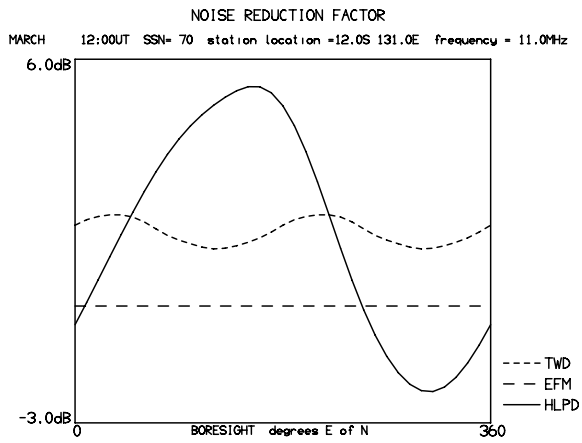

Figure 17. Midevening NRF for various antennas at Darwin.

EFM has a noise performance that is very little different from the CCIR monopole. Figure 16 shows the same site during midevening, from which it will be noted that the noise from Southeast Asia is now dominant. The worst performance for the HLPD is still toward the northwest, but there is a considerable improvement in virtually all other directions. In addition, there is a small improvement in the performance of the TWD. A further example is given in Figure 17, which shows the early evening NRF performance for antennas located at Darwin. It will be noted that there is considerable change in antenna performance from that exhibited at Alice Springs. This is a direct result of the greatly changed propagation conditions due to the proximity of the equatorial anomaly. In particular, it will be noted that there is a decreased performance

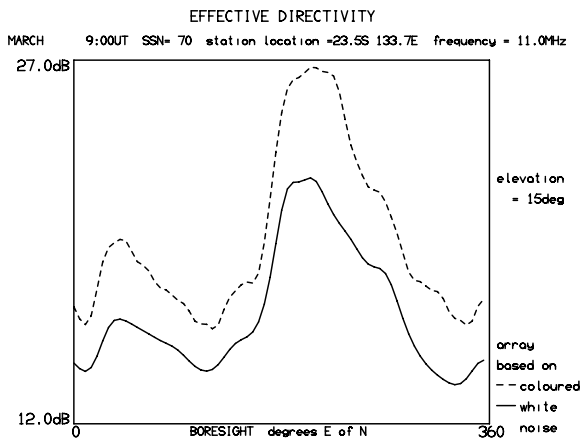

Figure 18. Comparison of effective gains for arrays based on white and colored noise.

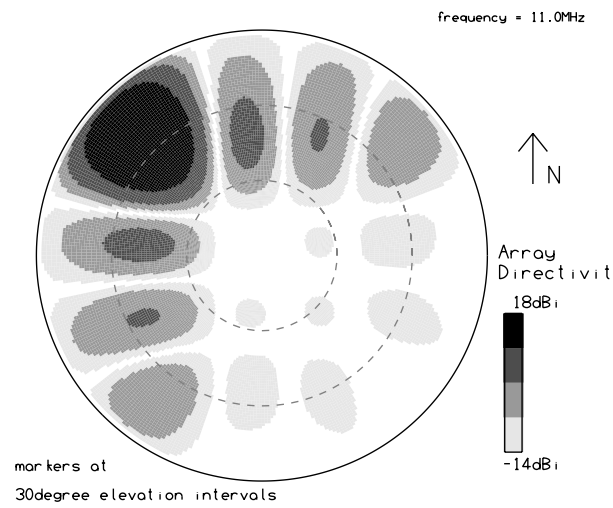

Figure 19. Directivity of a beam optimized on white noise.

in the TWD due to the greater amount of noise that enters through the higher elevation angles.

[13] A further issue arises when considering the reception of HF signals via an array-based antenna. Normal beam-forming weights are calculated by optimizing the SNR under the assumption that the noise is isotropic (directionally white). For HF this is clearly not the best approach, and the optimization should be based on direction-varying (colored) noise (see *Cox et al.* [1987] for examples of such beam-forming techniques). The impact of such an optimization can be seen in Figure 18, which shows the effective directivity (direc-

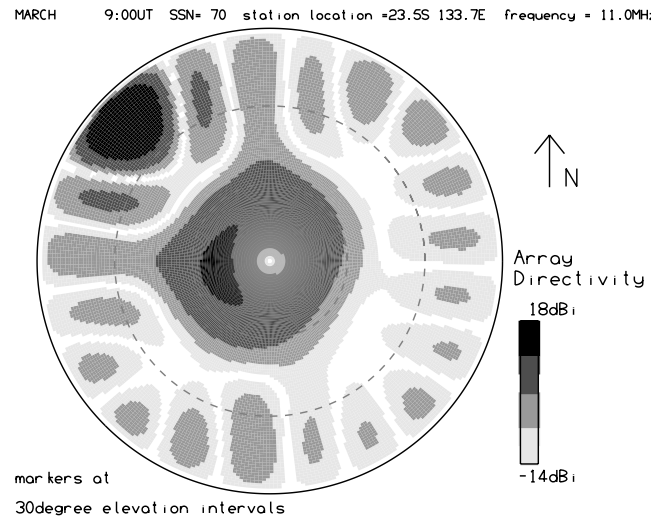

Figure 20. Directivity of a beam optimized on midevening colored noise.

tivity plus noise reduction factor) for an 6 × 6 array of monopole elements steered to an elevation of 15° and swept around through 360°. (The array elements were separated by 0.4 of a wavelength and, propagation conditions were the same as for Figure 5.) Also included is the effective gain that results when the beam forming is achieved by constant phase increments between elements in both array dimensions. It will be noted that there can be considerable improvement in effective gain (2 to 5 dB) when the directional noise distribution is used for optimization. Figures 19 and 20 show the directivity patterns of the arrays when the beam is steered toward the northeast. It will be noted from Figure 20 that the array based on colored noise achieves its increase in SNR by placing the sidelobes in directions where there is least noise (the higher elevations in particular).

[14] An important aspect of the validation of the current directional model has been the comparison of its predictions of total noise with those of the CCIR model (nonatmospheric contributions are taken from the CCIR model). *Kotaki* [1984] considered some representative examples for which noise observations were available. Table 1 shows some comparisons of effective antenna noise factor F_a for midevening at sites in Japan (36.5°N, 140.5°E), the United States (40.1°N, 105.1°W and 22.0°N, 159.7°W), Australia (30.6°S, 130.4°E), Sweden (59.5°, 17.3°E), and Singapore (1.3°S, 103.8°E). The midevening time is when the effects of atmospheric noise are at their strongest and so a good test of the models. Included in Table 1 are noise factor results derived from the CCIR model, the Kotaki model, the current model, and some observations. The effective antenna noise factor is defined by

$$F_a = 10 \log_{10} \left(\frac{P_n}{kT_0} \right),$$

where P_n is the noise collected by a lossless antenna in a 1 Hz bandwidth, k is the Boltzmann's constant, and T_0 is a reference temperature of 288 K.

Table 1. Comparison Between Observation and Noise Model Prediction for Various Locations Around the World[a]

Location	Frequency, MHz	CCIR F_a	*Kotaki* [1984] F_a	Current F_a	Observed F_a
35°N, 141°E	2.5	57	60	53	56
35°N, 141°E	5.0	50	51	53	54
35°N, 141°E	10.0	40	40	42	44
1°S, 104°E	2.5	68	66	63	61
31°S, 130°E	2.5	55	62	59	59
60°N, 17°E	2.5	51	56	57	52
22°N, 160°W	2.5	54	54	49	50
40°N, 105°W	2.5	60	61	57	60

[a] F_a values are given in decibels.

Table 2. Comparison Between Observation and Noise Model Prediction for Alice Springs[a]

Local Time	Current F_a	CCIR F_a	Observed F_a
1730	36	43	34
1900	45	46	45
2300	43	43	42

[a] F_a values are given in decibels.

[15] It will be noted that the predictions of the current model compare favorably with those of other models and perform significantly better than the CCIR model in several cases. Some comparisons with noise observations on a frequency of 10 MHz for a site near Alice Springs in central Australia (133.7°E, 23.5°S) are given in Table 2 (P. S. Whitham, private communication, 2000).

[16] It will be noted that the current model gives a fairly accurate representation of all the above observed results but that the CCIR model gives a significant overestimate at the time of the dusk terminator. (It should be noted that *Kotaki* [1984] also found situations where his model gave significantly better predictions than CCIR estimates of noise, as can be seen from Table 1.) In deriving the estimates of noise for comparison with the CCIR model it was necessary to add corrections due to the directive gain of the antenna used in the CCIR observations (a broadband monopole over a radial ground system). The low-elevation directive gains of this antenna were found to be quite sensitive to the nature of the ground under the antenna. Plausible variations in ground conductivity were found to cause several decibels of deviation in noise estimates for circumstances where there existed a large amount of low-elevation noise. As a consequence, it is likely that some of the seasonal variation in CCIR noise could be a result of variations in site conditions. In the current work, however, a representative value of 0.01 S/m was assumed for ground conductivity, and 15 was assumed for relative permittivity.

4. Conclusion

[17] The current paper has developed a model for the atmospheric component of noise at HF frequencies. Not only has this model given predictions that are in agreement with the standard CCIR model in most of the test cases, but it has also improved upon some of the anomalous predictions. More importantly, however, the model is able to address the issue of the directionality of noise. This issue has been shown to be extremely

important when considering the performance of antennas in receive applications. In particular, the directionality of noise, when coupled with the directionality of the antenna gain, can result in the system collecting an amount of noise that is greatly different from the isotropic case (the basis of CCIR estimates). In many cases the amount by which CCIR noise must be adjusted has been found to be quite large, and this serves to emphasize the need for consideration of noise directionality in HF system performance prediction.

[18] The directional noise model has been developed into a performance prediction model for HF systems. The model uses antenna gain patterns together with the directional distribution of noise in order to estimate the noise that enters the receiver. This is combined with propagation predictions and other system parameters in order to estimate the SNR that will be available at the receiver. At present, the noise estimates are based on median maps of thunderstorm activity and ionospheric parameters. As a consequence, the current model will only provide a median picture of noise that can, at best, provide the planner with a ''typical'' system behavior. In the future, however, it may be possible to use meteorological forecasts to provide more effective short-term predictions of thunderstorms [*Warber and Prasad*, 1997] and hence of noise. If these predictions are coupled with short-term forecasts of ionospheric behavior (based on ionosonde observations), it should be possible to derive effective short-term predictions of HF system performance.

[19] **Acknowledgments.** The author would like to thank referees for helpful comments.

References

Bilitza, D., International reference ionosphere 1990, *Rep. 90–22*, Natl. Space Sci. Data Cent., Greenbelt, Md., 1990.

Carhoun, D. O., Adaptive nulling and spatial spectral estimation using an iterated principle components decomposition, paper presented at IEEE International Conference on Acoustics, Speech and Signal Processing, IEEE Signal Process. Soc., Toronto, Canada, 1991.

Clarke, C., Atmospheric noise structure, *Electron. Technol.*, *37*, 197–204, 1960.

Coleman, C. J., On the simulation of backscatter ionograms, *J. Atmos. Sol. Terr. Phys.*, *59*, 2089–2099, 1997.

Coleman, C. J., A ray tracing formulation and its application to some problems in over-the-horizon radar, *Radio Sci.*, *33*, 1187–1197, 1998.

Coleman, C. J., The directionality of atmospheric noise and its impact upon an HF receiving system, in *Proceedings of the 8th International Conference on HF Radio Systems and Techniques*, *IEE Conf. Publ.*, *474*, 363–366, 2000.

Cox, H., R. M. Zeskind, and M. M. Owen, Robust adaptive beamforming, *IEEE Trans. Acoust. Speech Signal Process.*, *ASSP-35*, 1365–1375, 1987.

Davies, K., *Ionospheric Radio*, *IEE Electromagn. Waves Ser.*, vol. 31, Peter Peregrinus, London, 1990.

International Radio Consultative Committee (CCIR), World distribution and characteristics of atmospheric radio noise data, *Rep. 322*, Int. Radio Consult. Comm., Int. Telecommun. Union, Geneva, 1964.

International Telecommunication Union (ITU), Radio noise, *ITU-R Rep. P.372*, Geneva, 1999.

Jursa, A. S. (Ed.), *Handbook of Geophysics and the Space Environment*, Air Force Geophys. Lab., Air Force Syst. Command, U.S. Air Force, Bedford, Mass., 1985.

Keller, C. M., HF noise environment models, *Radio Sci.*, *26*, 981–995, 1991.

Kotaki, M., Global distribution of atmospheric radio noise derived from thunderstorm activity, *J. Atmos. Terr. Phys.*, *46*, 867–877, 1984.

Kotaki, M., and C. Katoh, The global distribution of thunderstorm activity observed by the Ionosphere Satellite (ISS-b), *J. Atmos. Terr. Phys.*, *45*, 833–850, 1984.

Lucas, D. L., and G. W. Haydon, Predicting statistical performance indexes for high frequency telecomunications systems, *ESSA Tech. Rep. IER 1-ITSA*, Natl. Oceanic and Atmos. Admin., Silver Spring, Md., 1966.

Warber, C. R., and B. Prasad, Forecasting global lightning for atmospheric noise prediction, *Radio Sci.*, *32*, 2027–2036, 1997.

C. J. Coleman, Electrical and Electronic Engineering Department, University of Adelaide, South Australia 5005, Australia. (ccoleman@eleceng.adelaide.edu.au)